

CLIP Behaves like a Bag-of-Words Model Cross-modally but not Uni-modally

Darina Koishigarina
 University of Tübingen
 Tübingen AI Center
 darina51012@gmail.com

Arnas Uselis
 University of Tübingen
 Tübingen AI Center

Seong Joon Oh
 University of Tübingen
 Tübingen AI Center

Abstract

CLIP (Contrastive Language-Image Pretraining) has become a popular choice for various downstream tasks. However, recent studies have questioned its ability to represent compositional concepts effectively. These works suggest that CLIP often acts like a bag-of-words (BoW) model, interpreting images and text as sets of individual concepts without grasping the structural relationships. In particular, CLIP struggles to correctly bind attributes to their corresponding objects when multiple objects are present in an image or text. In this work, we investigate why CLIP exhibits this BoW-like behavior. We find that the correct attribute-object binding information is already present in individual text and image modalities. Instead, the issue lies in the cross-modal alignment, which relies on cosine similarity. To address this, we propose Linear Attribute Binding CLIP or LABCLIP. It applies a linear transformation to text embeddings before computing cosine similarity. This approach significantly improves CLIP’s ability to bind attributes to correct objects, thereby enhancing its compositional understanding. The code is available at <https://github.com/kdarina/CLIP-not-BoW-unimodally>.

1. Introduction

Vision-language models (VLMs) like Contrastive Language-Image Pretraining (CLIP) [24] have achieved widespread adoption due to their shared embedding space for text and image modalities, which enables strong performance on various downstream tasks. However, a fundamental limitation has emerged: CLIP often struggles with compositionality [28], specifically the ability to bind attributes to corresponding objects in complex scenes [16, 27, 31]. Compositionality is essential for VLMs, as it allows models to generalize effectively by combining simpler concepts and understanding their relations.

Recent studies [31] have shown that CLIP frequently behaves like a bag-of-words (BoW) model, failing to bind attributes to corresponding objects. For instance, when pre-

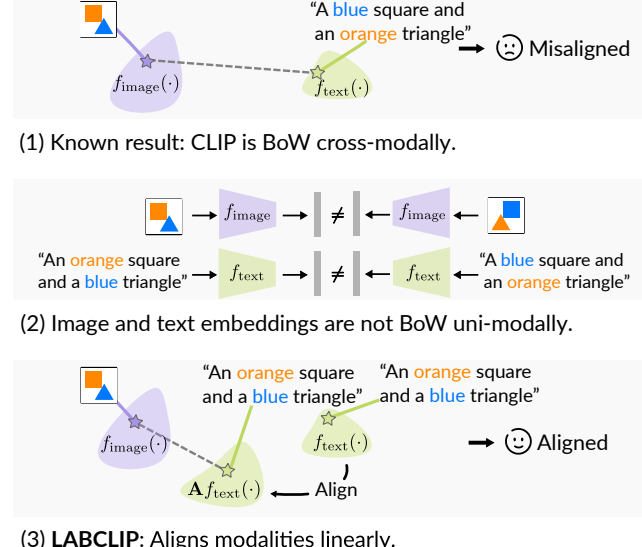


Figure 1. **LABCLIP mitigates the BoW behavior of CLIP.** (1) It has been reported that CLIP behaves like a BoW model with weak attribute-object binding. (2) We discover that embeddings of individual image and text modalities already contain the attribute-object binding information; this suggests that the cross-modal BoWness stems from the lack of alignment across the modalities. (3) A simple linear transformation of the text modality effectively mitigates the BoWness of CLIP.

sented with an image of “an orange square and a blue triangle” as in Figure 1, CLIP often matches the image to a caption “a blue square and an orange triangle”. It is often unable to distinguish the structural difference. We refer to this phenomenon as **BoWness**, indicating the model’s treatment of each data point as an unordered set of concepts. The BoWness significantly limits CLIP’s compositional understanding. Previous research has evaluated this limitation by jointly considering the image and text embeddings. However, there has been little investigation into the source of the inability. In particular, we do not know whether the BoWness arises (1) from a lack of attribute-object binding information in the individual text and image embeddings or

(2) from a mere lack of cross-modal alignment, achieved through cosine similarity.

In this work, we provide an answer to this question by measuring the presence of attribute-object binding information in individual image and text embeddings of CLIP. We train linear probes designed to extract attribute information for particular objects of interest. We then show that individual modalities linearly separate the attributes for each object present in the image or caption in almost any case. We thus verify that the embeddings of individual modalities contain the right attribute-object binding.

Building on this insight, we hypothesize that the CLIP’s BoWness is attributable to superficial misalignment stemming from the cosine similarity computation. To validate this, we propose Linear Attribute Binding CLIP, or **LAB-CLIP**, to align the text and image modalities with a simple linear transformation **A**. The linear transformation is trained with synthetic negative samples obtained by permuting attribute-object associations in text captions in image-caption datasets. The CLIP encoders remain frozen. Empirically, we demonstrate significant improvements in cross-modal attribute-object binding in multiple benchmarks including ARO, SugarCrepe, and COCO.

2. Related work

Limitations of CLIP’s Encoders. Numerous studies have highlighted weaknesses in both CLIP’s vision and text encoders. CLIP’s visual encoder tends to prioritize high-level understanding, often missing finer details crucial for distinguishing objects [30]. Meanwhile, its text encoder struggles with tasks involving negations, spatial and numerical reasoning, and nuanced attribute distinctions [13, 29]. These limitations affect performance in downstream applications [22, 29, 30]. Several efforts aim to interpret CLIP’s representations to understand these limitations better [5, 8, 32]. In contrast, our work specifically focuses on attribute-object binding in scenarios with multiple objects and attributes, providing a targeted analysis of its compositional capabilities.

Compositional Reasoning and Alignment. Compositional reasoning, critical for understanding complex scenes, has been studied extensively in neural networks [9, 11]. Prior work on CLIP investigates its ability to handle novel object-attribute combinations [1, 4] and attributes its failures to weak compositional reasoning [16, 27]. Some research employs controlled setups with two objects and distinct attributes [16, 27], providing initial insights into the attribute-object binding problem. Unlike these studies, our work examines whether CLIP’s architecture inherently limits its ability to bind attributes to objects by evaluating its capacity for capturing binding information within and across modalities.

Benchmarks for Compositionality. A growing number of

benchmarks evaluate compositionality in vision-language models, often using hard negatives or fine-grained distractors to challenge CLIP’s compositional reasoning [10, 19, 25, 28, 31, 33]. These benchmarks vary in focus: some test fine-grained distinctions [3], others use hard positive pairs for reasoning [15], and some target specific challenges like counting [21] or spatial reasoning [14]. Additionally, synthetic benchmarks provide controlled environments to test compositional reasoning with targeted scenarios often missing in real-world datasets [6, 12]. Our work extends these efforts by contributing a synthetic, controlled dataset with greater variation, specifically designed to evaluate attribute-object binding.

3. The binding problem

Ideally, vision-language models like CLIP need to capture the compositional structure of real-world scenes. A necessary condition for compositional understanding is the ability to accurately bind attributes to corresponding objects in scenes with multiple objects. Prior research suggests that CLIP’s attribute-object binding is often arbitrary to the degree that the model can effectively be thought of as a bag-of-words (BoW) extractor that treats objects and attributes in image and text as an unordered collection of concepts, completely ignoring the order and structure therein [31].

In this work, we define **BoWness** of a vision-language model as the general tendency in models to treat inputs (image or text) as unordered sets of concepts. In contrast, we say that a model has a **binding ability** when it can link attributes correctly to the corresponding objects.

3.1. Preliminaries

A CLIP model includes two feature extractors: $f_{\text{image}} : \mathcal{I} \rightarrow \mathbb{R}^D$ for images and $f_{\text{text}} : \mathcal{T} \rightarrow \mathbb{R}^D$ for texts, where D is the dimensionality of CLIP encoders. For an image $\mathbf{x}^{\text{img}} \in \mathcal{I}$ and a text sequence $\mathbf{x}^{\text{txt}} \in \mathcal{T}$, CLIP embeds both inputs independently into a shared vision-language space. We are interested in the behavior and information content in embeddings $f_{\text{text}}(\mathbf{x}^{\text{txt}})$ and $f_{\text{image}}(\mathbf{x}^{\text{img}})$ for a language-image pair $(\mathbf{x}^{\text{img}}, \mathbf{x}^{\text{txt}})$.

We consider a paired image-text dataset $\mathcal{D} = \{(\mathbf{x}_i^{\text{img}}, \mathbf{x}_i^{\text{txt}})\}_{i=1}^N$ of N samples, where each sample consists of a text sequence $\mathbf{x}_i^{\text{txt}} \in \mathcal{T}$ and a corresponding image $\mathbf{x}_i^{\text{img}} \in \mathcal{I}$. Such a dataset typically provides abundant *positive pairs* with correct associations of attributes in the text captions to objects in the corresponding images. We refer to *negative pairs* as synthetic pairs where the text captions in positive pairs are modified in a way that the attribute-object association is artificially broken through a permutation. For example, given a positive pair with the caption “a red cube and a blue sphere”, we create a negative pair by keeping the image intact and modifying the caption to “a blue cube and a red sphere”.

The creation and usage of such synthetic negative pairs have been an established strategy in the assessment of CLIP’s ability to differentiate correct and incorrect attribute-object binding, as seen in previous benchmarks [10, 28, 31]. Other researchers have considered incorporating the negative pairs in training or fine-tuning CLIP to further equip the model with improved attribute-object binding [23, 31]. Our work, likewise, employs negative pairs for assessing and improving CLIP.

3.2. Datasets

In evaluating CLIP’s ability to perform attribute-object binding, we start by considering established real-world benchmarks that are commonly used to test compositional understanding in vision-language models.

ARO [31] is a benchmark that tests compositionality in VLMs using real-world images, specifically evaluating their ability to understand different types of relationships, attributes, and order information.

SugarCrepe [10] is a benchmark for evaluating compositional understanding in vision-language models by generating fluent and sensible hard negatives.

COCO [18] is a large-scale dataset containing diverse scenes and object categories used to evaluate object recognition, segmentation, and image captioning in complex real-world scenarios.

While these benchmarks offer insights into cross-modal alignment, their complexity and large variety of objects make them unsuitable for systematic evaluation of uni-modal attribute-object binding. Cross-modal binding only requires matching images to text, making it manageable despite the variability. However, for uni-modal binding, we need a controlled set of attributes and objects with consistent examples to assess how well the model links attributes to objects within a single modality. Due to this lack of control, real-world datasets are inadequate for testing uni-modal binding and are primarily suited to cross-modal alignment.

To overcome this, we use synthetic datasets. They provide exact control over objects and their attributes. This control allows for more targeted assessments of compositional behavior.

CLEVR [12] is a synthetic dataset featuring simple shapes and colors, offering a highly controlled environment to examine attribute-object binding without the complexities of natural scenes.

PUG:SPAR [6] is a synthetic dataset that extends the idea of controlled settings by using animal figures in varied scenes. PUG aims to introduce a more realistic context while retaining control over attributes. SPAR stands for four variations present in the dataset: Scene, Position, Attribute, and Relation. See Figure 2 for examples.

A remaining limitation of PUG:SPAR for the analysis of

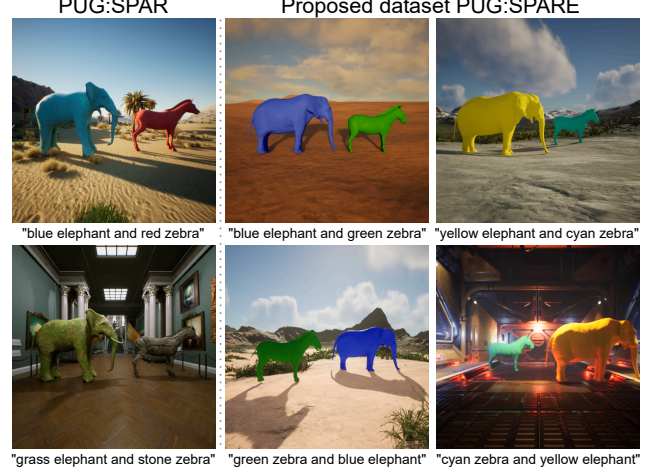


Figure 2. **Comparison of examples from PUG:SPAR [6] and PUG:SPARE.** In PUG:SPAR, attributes correlated with object positions: objects on the left are linked to “blue” or “grass” and objects on the right are “red” or “stone”. Our dataset PUG:SPARE de-correlates the potential shortcut.

attribute-object binding is the presence of positional biases, where specific attributes are consistently correlated with the object positions (e.g., objects on the left are always blue or grass, and those on the right are red or stone). This opens up shortcuts through which models may achieve superficial attribute-object binding, while not genuinely understanding the structure.

PUG:SPARE is our modification of PUG:SPAR that mitigates the positional shortcut (Figure 2). ‘E’ stands for ‘Extended’. PUG:SPARE randomizes the attribute-object associations across positions, ensuring that models may not exploit spatial bias. This modification allows for a more accurate assessment of CLIP’s compositional capabilities. The details about the dataset generation are provided in the Appendix.

We use ARO, SugarCrepe and COCO in Section 4. We use CLEVR, PUG:SPAR and PUG:SPARE in Sections 3.3, 3.4, and 4.

3.3. CLIP is a bag-of-words cross-modally

In this section, we explain how previous approaches demonstrated the bag-of-words nature of CLIP. We reproduce prior results and confirm that CLIP is BoW cross-modally.

Previous approach demonstrating BoWness. A common approach to demonstrate CLIP’s BoWness behavior is by comparing the embeddings of an image with permutations of its caption [31]. For example, given an image of an orange square and a blue triangle, possible captions could be “an orange square and a blue triangle” and “an orange triangle and a blue square”. The task is to identify the correct caption from these options, where one has correct color-

object associations and the other has swapped associations. CLIP’s prediction is based on which caption embedding has a higher cosine similarity with the image embedding.

Ideally, CLIP should exhibit **cross-modal binding**, or an accurate association of attribute-object pairs across modalities. However, CLIP has been reported to be **cross-modally BoW**, treating the concepts in inputs as an unordered collection. These two opposite cases manifest as the correctness of the ranking of cosine similarities for pairs of inputs, as shown in the figure below.

Cross-modally BoW:

$$f_{\text{image}}(\text{orange square, blue triangle})^\top f_{\text{text}}(\text{"an orange square and a blue triangle"}) \\ \approx f_{\text{image}}(\text{orange triangle, blue square})^\top f_{\text{text}}(\text{"an orange triangle and a blue square"})$$

Cross-modal binding:

$$f_{\text{image}}(\text{orange square, blue triangle})^\top f_{\text{text}}(\text{"an orange square and a blue triangle"}) \\ > f_{\text{image}}(\text{orange triangle, blue square})^\top f_{\text{text}}(\text{"an orange triangle and a blue square"})$$

Replicating BoWness results. Using this approach on the datasets discussed previously, *our results confirm prior findings*, with accuracy levels close to chance. Specifically, we observe *0.56 accuracy on CLEVR, 0.51 on PUG:SPAR, and 0.50 on PUG:SPARE*, indicating that CLIP’s performance is virtually at the level of random guessing. These results strongly suggest that CLIP cannot distinguish between correct and permuted attribute-object bindings. CLIP is indeed a bag-of-words model.

3.4. CLIP binds concepts unimodally

Prior works evaluating CLIP’s BoW tendencies have relied on assessments that combine both text and image modalities. This approach has a key limitation: it does not separate the encoding of attribute-object binding within each modality from the cross-modal matching step. As a result, it remains unclear whether CLIP’s BoW behavior stems from limitations in the embeddings themselves or from issues in cross-modal alignment. To address this, we examine the **uni-modal binding**, referring to CLIP’s ability to encode attribute-object relationships independently within each modality. By evaluating text and image embeddings separately, we aim to clarify whether each modality alone captures sufficient binding information, shedding light on the roots of CLIP’s BoW behavior.

Linear probing for uni-modal binding. To evaluate if CLIP encodes binding information within each modality, we use linear probing [2]. By training linear classifiers for the information we care about on top of frozen representations, we assess the existence of information we seek in the representation. In this case, we seek the attribute-object binding information in each modality; we train linear classifiers separating attributes for each object present in the image or text inputs.

Given a dataset $\mathcal{D} = \{(\mathbf{x}_i^{\text{img}}, \mathbf{x}_i^{\text{txt}})\}_{i=1}^N$, we define \mathcal{O} as

the set of all objects and \mathcal{A} as the set of all attributes in the dataset. For each object $o \in \mathcal{O}$, we train two separate classifiers, one for images and one for text as shown in Fig. 3. These classifiers are trained using embeddings extracted by the respective CLIP encoders, which remain frozen throughout the training process. We denote object-specific probes as image-probe_o and text-probe_o , each predicting the attribute $a \in \mathcal{A}$ for the object o based on either image or text embeddings:

$$\text{image-probe}_o : f_{\text{image}}(\mathbf{x}_i^{\text{img}}) \mapsto a \\ \text{text-probe}_o : f_{\text{text}}(\mathbf{x}_i^{\text{txt}}) \mapsto a. \quad (1)$$

For example, as illustrated in Fig. 3(a), given an image or text describing a scene with “a blue cylinder and red cube” we extract corresponding embeddings using the CLIP encoders. We then train a linear classifier to recognize the attribute (e.g. $a = \text{"red"}$) of a specific object (e.g. $o = \text{"cube"}$). This process allows us to isolate and probe attribute recognition for each object individually within each modality.

We measure the amount of attribute-object binding information in each modality by evaluating the validation-set accuracy of the linear probes for the attribute prediction task. We measure the average attribute prediction accuracy across all objects $o \in \mathcal{O}$. It essentially measures the linear separability of the attributes for each object in the CLIP representations for each modality. To contextualize the information content in pre-trained CLIP representations, we provide accuracies of random baseline and CLIP encoders fine-tuned for the attribute prediction task. They provide the reference points for no binding information and maximal binding information in the encoders, respectively. See Appendix for further details.

Results. Table 1 presents the attribute classification accuracies for the linear probes on text and image representations for datasets CLEVR, PUG:SPAR, and PUG:SPARE. The linear probes trained on pre-trained CLIP embeddings achieve accuracies far beyond the random baseline for both image (e.g. 0.96 on image-test set compared to 0.12 for CLEVR) and text (e.g. 1.00 on text-test vs to 0.12 for random) modalities. The accuracies are close to the maximal information bound given by the fine-tuned CLIP encoders.

Sanity check: BoW models lack discriminative signal. As a sanity check, we confirm that a truly BoW representation lacks the structure necessary for attribute-object binding. We train randomly initialized CLIP encoders under a BoW constraint, ensuring they recognize all attributes in an input without the constraint to associate them with objects. This is implemented by training both encoders to predict the presence of each attribute using soft label cross-entropy loss. We perform this for two-object case on CLEVR.

Applying linear probing to the resulting embeddings reveals significantly worse accuracy compared to the original CLIP embeddings (0.66 for images, 0.85 for text vs.

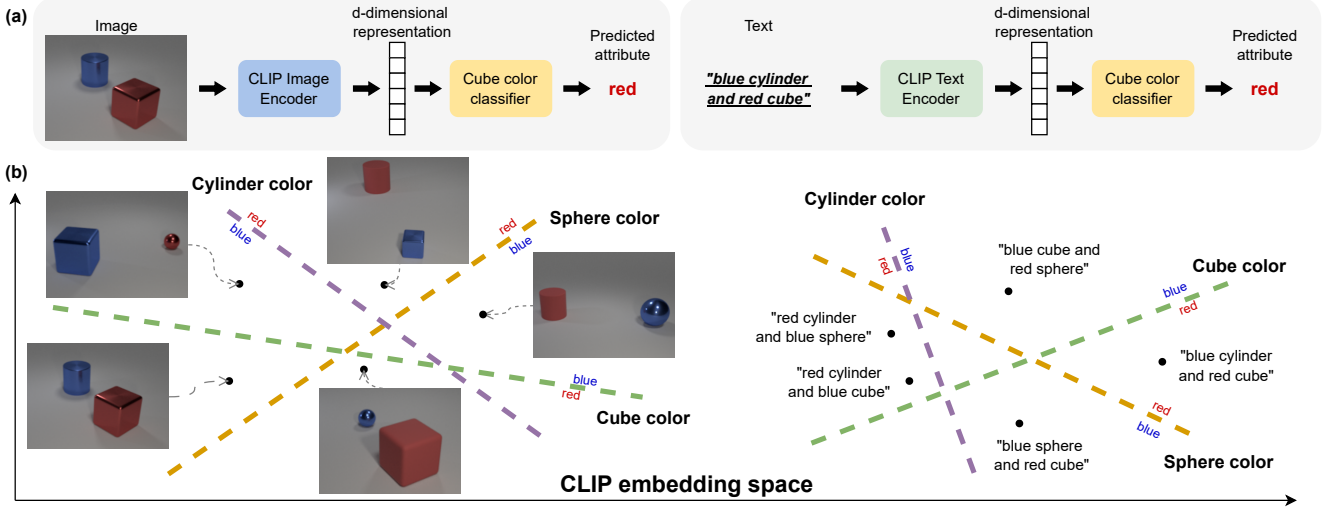


Figure 3. **Uni-modal attribute-object binding.** (a) we train a linear probe per object to distinguish its color within image and text modality separately. (b) the linear probe establishes decision boundaries in CLIP’s representation space that differentiate between various attribute-object associations.

Dataset	Encoder	Image		Text	
		Train	Test	Train	Test
CLEVR	Random	0.12	0.12	0.12	0.12
	CLIP	1.00	0.96	1.00	1.00
	CLIP (ft)	1.00	0.99	1.00	1.00
PUG:SPAR	Random	0.25	0.25	0.25	0.25
	CLIP	1.00	0.99	1.00	0.99
	CLIP (ft)	1.00	0.98	1.00	1.00
PUG:SPARE	Random	0.12	0.12	0.12	0.12
	CLIP	0.99	0.95	1.00	1.00
	CLIP (ft)	1.00	1.00	1.00	1.00

Table 1. **CLIP is not BoW uni-modally.** We measure the amount of attribute-object binding information in image and text representations for CLIP. Accuracies of linear probes classifying attributes for each object of interest are shown. Performances based on random baseline and fine-tuned (ft) CLIP encoders provide reference points for minimal and maximal binding information, respectively. We observe that pre-trained CLIP encoders have sufficient attribute-object binding information in respective modalities.

0.96 for CLIP). This confirms that a BoW model does not retain meaningful discriminative signals, illustrating that high-dimensional representations by themselves may fail to encode binding information in the absence of object-specific information.

We conclude that CLIP is already aware of attribute-object bindings in individual modalities. We hypothesize that CLIP’s BoW behavior [16, 27] stems from the poor cross-modal alignment that takes place after the encoding stage. We verify the hypothesis in the next section.

4. Improving cross-modal binding

We have observed in the previous section that CLIP is not a bag-of-words (BoW) model uni-modally, suggesting the existence of the necessary attribute-object binding information in individual modalities. We thus narrow down the root cause of the previously observed cross-modal BoWness to a poor cross-modal alignment in the representation space. In this section, we verify that this is indeed the case by proposing a simple alignment strategy that recovers the attribute-object binding information across the modalities. Specifically, we propose to apply a simple linear transformation on the embeddings of one of the modalities (e.g. text) to ensure that the cosine similarities retrieve pairs with correct binding first. We refer to this method as LABCLIP.

4.1. Linear Attribute Binding CLIP

Linear Attribute Binding CLIP (LABCLIP) trains a linear transformation to better align the text and image embeddings. Instead of the standard image-text matching in CLIP,

$$\langle f_{\text{image}}(\mathbf{x}^{\text{img}}), f_{\text{text}}(\mathbf{x}^{\text{txt}}) \rangle,$$

LABCLIP applies a transformation matrix $\mathbf{A} \in \mathbb{R}^{D \times D}$ on the text embeddings before the inner product computation:

$$\langle f_{\text{image}}(\mathbf{x}^{\text{img}}), \mathbf{A} f_{\text{text}}(\mathbf{x}^{\text{txt}}) \rangle.$$

Training. We train the linear transformation matrix \mathbf{A} contrastively, mirroring CLIP’s original training setup. Two approaches are explored: **Standard Batch (SB)**, which uses a batch of B positive image-text pairs; and **Hard Negative Batch (HNB)**, which includes negative text samples

within the batch, following [31]. Negative samples are created by permuting the concepts in the original captions. For example, we transform “a photo of a red cube and a blue sphere” into “a photo of a blue cube and a red sphere” without changing the image part. Such negative samples can be generated without extra annotation costs. We denote a function performing such permutations as

$$\text{permute} : \mathcal{T} \rightarrow \mathcal{T}.$$

The captions in COCO are not structured in a straightforward “attribute-object” format, making it challenging to isolate and swap attributes and objects directly. Because of this, we use the NegCLIP strategy from [31], which shuffles nouns and adjectives to create negative samples. In training, including negative text samples results in a $B \times 2B$ batch, where the transformation is used to minimize the similarity with mismatched attribute-object pairs. The training process of LABCLIP is illustrated in Algorithm 1.

CLIP’s weights remain frozen for LABCLIP. For a reference point, we also provide results with a fine-tuned CLIP model, denoted CLIP-FT. For all the considered methods and their variations, we perform only minimal hyperparameter searches and select models based on the validation set results at the last epoch. Unless stated otherwise, we use the approach with Hard Negative Batch as the default version of LABCLIP. See Appendix for a detailed description of the experimental setup.

Algorithm 1 Training algorithm for Linear Attribute Binding CLIP (LABCLIP)

```

1: Initialize transformation matrix  $\mathbf{A} \in \mathbb{R}^{D \times D}$ 
2: Precompute  $\mathbf{i}_i = f_{\text{image}}(\mathbf{x}_i^{\text{img}})$  and  $\mathbf{t}_i = f_{\text{text}}(\mathbf{x}_i^{\text{txt}})$  for all  $i$  (CLIP encoders frozen)
3: for epoch = 1 to  $N_{\text{epochs}}$  do
4:   for each batch  $\{(\mathbf{i}_i, \mathbf{t}_i)\}_{i=1}^B$  do
5:      $\mathbf{t}_{i,\text{pos}} = \mathbf{A}\mathbf{t}_i$ 
6:     Compute positive scores  $s_{i,i} = \langle \mathbf{i}_i, \mathbf{t}_{i,\text{pos}} \rangle$ 
7:     if negative sampling then
8:       Generate negatives:  $\mathbf{t}_{j,\text{neg}} = \mathbf{A} f_{\text{text}}(\text{permute}(\mathbf{x}_j^{\text{txt}}))$ 
9:       Compute negative scores  $s_{i,j} = \langle \mathbf{i}_i, \mathbf{t}_{j,\text{neg}} \rangle$  for  $i \neq j$ 
10:      Effective batch size:  $B \times 2B$ 
11:      Compute  $\mathcal{L}_{\text{img-to-txt}} = \text{CE}(\{s_{i,i}\}, \{s_{i,j}\})$ 
12:      Compute  $\mathcal{L}_{\text{txt-to-img}} = \text{CE}(\{s_{i,i}\}, \{s_{j,i}\})$ 
13:       $\mathcal{L} = \mathcal{L}_{\text{img-to-txt}} + \mathcal{L}_{\text{txt-to-img}}$ 
14:      Update  $\mathbf{A}$  to minimize  $\mathcal{L}$ 
15: Return learned transformation matrix  $\mathbf{A}$ 

```

4.2. Results

Table 2 provides the cross-modal binding results on CLEVR, PUG:SPAR, and PUG:SPARE. The first column indicates the accuracy of a model in matching an image to one of two options: the correct caption or the caption with

	Accuracy		Recall@1	
	Train	Test	Train	Test
CLEVR				
- Random	0.50	0.50	0.01	0.01
- CLIP	0.49	0.58	0.25	0.36
- LABCLIP-SB	1.00	0.95	1.00	0.94
- LABCLIP-HNB	1.00	0.95	1.00	0.93
- CLIP-FT	1.00	1.00	0.99	0.97
PUG:SPAR				
- Random	0.50	0.50	0.00	0.00
- CLIP	0.52	0.53	0.08	0.09
- LABCLIP-SB	1.00	0.97	0.98	0.90
- LABCLIP-HNB	1.00	0.97	0.98	0.91
- CLIP-FT	1.00	1.00	1.00	0.99
PUG:SPARE				
- Random	0.50	0.50	0.00	0.00
- CLIP	0.50	0.50	0.06	0.06
- LABCLIP-SB	0.94	0.90	0.90	0.86
- LABCLIP-HNB	0.98	0.94	0.95	0.90
- CLIP-FT	1.00	1.00	1.00	1.00

Table 2. **LABCLIP recovers cross-modal binding.** We measure CLIP’s ability to rank correctly attribute-object relationships higher. Compared to the baseline CLIP, which exhibits close-to-random accuracies and R@1 performances, LABCLIP demonstrates a superior attribute-object binding by employing a single linear transformation on the text embeddings.

permuted attributes. Recall@1 measures the model’s ability to retrieve the correct caption for a given image from all possible captions in the dataset.

Without training, the original CLIP results are at the random chance level, as discussed in Section 3.3: CLIP cannot differentiate between correct and permuted captions cross-modally. Fine-tuning with negative samples enables perfect accuracy and near-perfect retrieval on these datasets, providing an upper bound on the possible attribute-object binding performance.

We observe that both alignment with the standard batch of samples (LABCLIP-SB) and with additional negative samples (LABCLIP-HNB) significantly improve performance compared to CLIP. On CLEVR, for example, both LABCLIP-SB and LABCLIP-HNB achieve an accuracy of 0.95, significantly greater than CLIP’s 0.58. The results suggest that better cross-modal binding can be achieved by linearly transforming one of the embedding spaces—text in our case—without requiring extensive computations, complex methodologies, or *any change to CLIP parameters*. This further corroborates our previous findings that all the ingredients and information for attribute-object binding are already present in the pre-trained CLIP models.

Table 3 demonstrates the performance of our method on the real-world data benchmarks, ARO [31] and Sugar-

Model	Backbone	ARO				SugarCrepe			COCO
		VG-A	VG-R	Flickr-PRC	COCO-PRC	Add	Replace	Swap	Recall@1
CLIP	ViT-B/32	0.63	0.63	0.60	0.48	0.73	0.80	0.62	0.30
NegCLIP [31]	ViT-B/32	0.71	0.81	0.91	0.86	0.87	0.85	0.75	0.41
LABCLIP-SB	ViT-B/32	0.64	0.59	0.42	0.32	0.83	0.83	0.69	0.41
LABCLIP-HNB	ViT-B/32	0.69	0.82	0.84	0.81	0.81	0.82	0.74	0.41
CLIP	ViT-B/16	0.62	0.56	0.58	0.50	0.73	0.80	0.62	0.33
LABCLIP-SB	ViT-B/16	0.60	0.57	0.41	0.32	0.84	0.84	0.67	0.44
LABCLIP-HNB	ViT-B/16	0.60	0.71	0.87	0.84	0.83	0.84	0.73	0.44
CLIP	ViT-L/14	0.63	0.64	0.55	0.47	0.75	0.79	0.61	0.37
LABCLIP-SB	ViT-L/14	0.62	0.60	0.44	0.31	0.85	0.84	0.64	0.46
LABCLIP-HNB	ViT-L/14	0.67	0.80	0.88	0.87	0.83	0.84	0.70	0.47

Table 3. **LABCLIP enhances compositional reasoning on real-world benchmarks.** We compare the performance of our method with baseline CLIP and fine-tuned CLIP with negative examples (NegCLIP) on compositional benchmarks ARO and SugarCrepe, as well as retrieval performance on COCO. The simple linear alignment matrix effectively transforms the CLIP representation space, improving attribute-object binding and compositional understanding.

Crepe [10], when trained on the COCO dataset [18]. Our method significantly outperforms the standard CLIP model, indicating better understanding of attributes, relations, and word order, which leads to improved compositional reasoning.

We compare these results to NegCLIP, a fine-tuned CLIP model with negative image and text samples from COCO [31]. It should be noted that, in contrast to NegCLIP, LABCLIP does not include *hard negative image data* in the batches and only uses one type of perturbation: shuffling of adjectives and nouns. Most importantly, our approach achieves comparable results to NegCLIP without requiring a computationally expensive fine-tuning process.

As discussed in [31], it has been suggested that CLIP’s design may lack the ability to differentiate between complex scenes and their subtle variations. Its bag-of-words behavior was sufficient for high retrieval performance without strong reasoning. However, our results indicate that CLIP’s representations might already contain information about attribute-object bindings. By training an additional linear layer contrastively, we show that this information can be aligned more effectively. This supports the idea that CLIP’s embeddings capture more compositional details than previously thought.

5. Analysis

In this section, we analyze the robustness of uni-modal binding with the increasing number of objects, the representational similarities before and after alignment, and the effect of alignment on the modality gap.

5.1. Uni-modal binding with more objects

To evaluate the robustness of CLIP’s uni-modal attribute-object binding capabilities, we extend the experiments in Section 3.4 by varying the number of objects in each scene. In this setup, we increase the object count within the CLEVR dataset and measure the attribute probing accuracy of linear classifiers trained to identify object-specific attributes in both image and text representations. The goal is to assess how robust CLIP’s attribute-object binding remains as the number of objects in the scene increases.

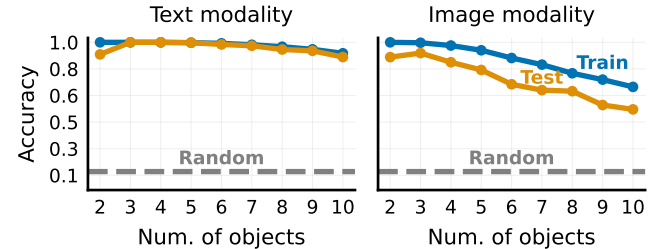


Figure 4. **Image and text embeddings effectively encode multiple objects.** We show the average linear probing accuracy on CLEVR as the number of objects increases. While performance slightly decreases, it remains relatively robust.

Figure 4 shows the attribute probing accuracy as a function of object count for both text and image modalities. The text modality maintains high accuracy, consistently above 0.8 across increasing object counts, indicating stable uni-modal binding for text representations. In contrast, the image modality’s accuracy declines with more objects: training accuracy drops from nearly 1.0 to around 0.75, and test accuracy falls from about 0.9 to 0.6 as the object count increases. These results suggest that while CLIP’s text em-

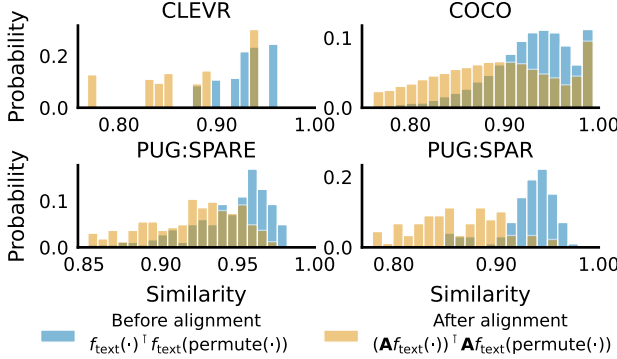


Figure 5. **Alignment reduces the similarity between permuted text pairs.** We show the distributions of cosine similarity between original and permuted text, before and after alignment.

beddings capture attribute-object bindings robustly, binding information in image embeddings degrades as scenes become more complex.

5.2. Representational similarities and alignment

To gain deeper insights into the impact of our alignment transformation, we analyze cosine similarity distributions between positive and negative pairs before and after applying the alignment matrix \mathbf{A} . For a text sequence \mathbf{x}^{txt} , the aligned text representation is given by $\mathbf{A}f_{\text{text}}(\mathbf{x}^{\text{txt}})$, where \mathbf{A} is the alignment transformation applied to the original CLIP text embedding $f_{\text{text}}(\mathbf{x}^{\text{txt}})$.

Text-to-text similarity. First, we consider cosine similarities between positive and negative text representations before alignment, $\langle f_{\text{text}}(\mathbf{x}_i^{\text{txt}}), f_{\text{text}}(\text{permute}(\mathbf{x}_i^{\text{txt}})) \rangle_{i=1}^N$, and after alignment, $\langle \mathbf{A}f_{\text{text}}(\mathbf{x}_i^{\text{txt}}), \mathbf{A}f_{\text{text}}(\text{permute}(\mathbf{x}_i^{\text{txt}})) \rangle_{i=1}^N$.

The distributions are depicted in Fig. 5. We observe that, before alignment, the similarities are higher, indicating that image embeddings may be incorrectly matched with permuted text embeddings. After alignment, positive and negative text pairs become more dissimilar, potentially making it easier to distinguish between permuted text pairs.

Image-to-text similarity. We analyze cross-modal similarities by comparing image embeddings to both positive and negative text embeddings, as shown in Fig. 6. The solid bars represent similarities between image embeddings and text embeddings for positive pairs $\langle f_{\text{image}}(\mathbf{x}_i^{\text{img}}), f_{\text{text}}(\mathbf{x}_i^{\text{txt}}) \rangle_{i=1}^N$ and negative pairs $\langle f_{\text{image}}(\mathbf{x}_i^{\text{img}}), f_{\text{text}}(\text{permute}(\mathbf{x}_i^{\text{txt}})) \rangle_{i=1}^N$ before alignment.

The results indicate no distinction between positive and negative pairs before alignment, as the solid bars for both are at the same height. However, after alignment (dashed bars), the similarity to positive text embeddings $\langle f_{\text{image}}(\mathbf{x}_i^{\text{img}}), f_{\text{text}}(\mathbf{A}\mathbf{x}_i^{\text{txt}}) \rangle_{i=1}^N$ is notably higher than to permuted text $\langle f_{\text{image}}(\mathbf{x}_i^{\text{img}}), f_{\text{text}}(\mathbf{A}\text{permute}(\mathbf{x}_i^{\text{txt}})) \rangle_{i=1}^N$. This demonstrates that alignment enables better differentiation,

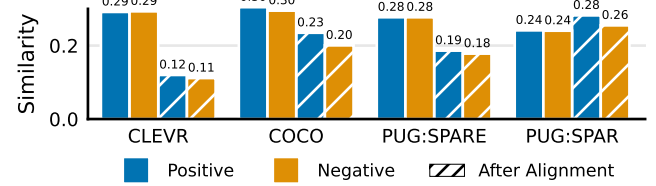


Figure 6. **LABCLIP enhances the similarity between image representation and correct text representations** We show the similarity distributions between image representations to positive and negative text representations before and after alignment.

allowing the model to match images with the correct text rather than the permuted text.

5.3. Implications to modality gap

A key challenge in multimodal models like CLIP is the modality gap—a discrepancy between vision and text embeddings [17]. Previous studies [26] suggest that reducing this gap improves alignment and interaction between modalities. Motivated by this, we measure the Euclidean distance between mean embeddings \mathbf{x} and \mathbf{y} from the vision and text representations before and after alignment. Specifically, we define $\mathbf{x} := \frac{1}{N} \sum_{i=1}^N f_{\text{image}}(\mathbf{x}_i)$ and $\mathbf{y} := \frac{1}{N} \sum_{i=1}^N f_{\text{text}}(\mathbf{y}_i)$, where f_{image} and f_{text} denote the encoders, and N is the sample size. We then compute $\|\mathbf{x} - \mathbf{y}\|_2$ for original embeddings and $\|\mathbf{x} - \mathbf{A}\mathbf{y}\|_2$ for aligned embeddings, where \mathbf{A} is a contrastively trained alignment matrix using LABCLIP.

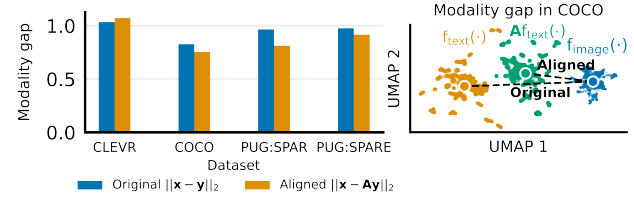


Figure 7. **Modality gap decreases after alignment.** Left: Modality gap between image and text representations before and after alignment. Right: UMAP visualization of COCO test set representations with text representations before and after alignment.

Our experiments reveal that the modality gap decreases substantially across COCO, PUG:SPAR, and PUG:SPARE datasets after alignment, while CLEVR shows a slight increase (Fig. 7, left). Additionally, we provide a qualitative illustration of the modality gap (Fig. 7, right) using UMAP [20] showing COCO test set representations before and after alignment. In this visualization, the aligned text representations (green) move closer to the image representations (blue), indicating reduced modality gap after alignment.

This suggests that alignment effectiveness may vary across datasets, with our approach successfully enhancing cross-modal compatibility in most cases.

6. Conclusion

In this study, we investigated the underlying reasons for CLIP’s bag-of-words behavior. We focused specifically on attribute-object binding. Our findings demonstrate that a substantial amount of attribute-object binding information is already present in CLIP’s text and image embeddings. The issue, instead, lies in the cross-modal alignment that relies on cosine similarity. To address this, we introduced LABCLIP, a method that applies a linear transformation to text embeddings. LABCLIP significantly improves attribute-object binding during cross-modal matching, enhancing compositional understanding without requiring modifications to the CLIP encoders. Our work motivates further exploration into contrastive training objectives, alignment processes, and the strategic use of hard negatives to enable CLIP to capture compositional relationships more robustly.

7. Acknowledgments

The authors thank the International Max Planck Research School for Intelligent Systems (IMPRS-IS) for supporting Arnas Uselis. This work was supported by the Tübingen AI Center.

References

- [1] Reza Abbasi, Mohammad Hossein Rohban, and Mahdieh Soleymani Baghshah. Deciphering the role of representation disentanglement: Investigating compositional generalization in clip models. *arXiv preprint arXiv:2407.05897*, 2024. [2](#)
- [2] Guillaume Alain. Understanding intermediate layers using linear classifier probes. *arXiv preprint arXiv:1610.01644*, 2016. [4](#)
- [3] Rabiul Awal, Saba Ahmadi, Le Zhang, and Aishwarya Agrawal. Vismin: Visual minimal-change understanding. *arXiv preprint arXiv:2407.16772*, 2024. [2](#)
- [4] Wentao Bao, Lichang Chen, Heng Huang, and Yu Kong. Prompting language-informed distribution for compositional zero-shot learning. *arXiv preprint arXiv:2305.14428*, 2023. [2](#)
- [5] Usha Bhalla, Alex Oesterling, Suraj Srinivas, Flavio P Calmon, and Himabindu Lakkaraju. Interpreting clip with sparse linear concept embeddings (splice). *arXiv preprint arXiv:2402.10376*, 2024. [2](#)
- [6] Florian Bordes, Shashank Shekhar, Mark Ibrahim, Diane Bouchacourt, Pascal Vincent, and Ari Morcos. Pug: Photorealistic and semantically controllable synthetic data for representation learning. *NIPS*, 36, 2024. [2, 3, 1](#)
- [7] Blender Online Community. *Blender - a 3D modelling and rendering package*. Blender Foundation, Stichting Blender Foundation, Amsterdam, 2018. [1](#)
- [8] Reza Esfandiarpoor, Cristina Menghini, and Stephen H Bach. If clip could talk: Understanding vision-language model representations through their preferred concept descriptions. *arXiv preprint arXiv:2403.16442*, 2024. [2](#)
- [9] Klaus Greff, Sjoerd Van Steenkiste, and Jürgen Schmidhuber. On the binding problem in artificial neural networks. *arXiv preprint arXiv:2012.05208*, 2020. [2](#)
- [10] Cheng-Yu Hsieh, Jieyu Zhang, Zixian Ma, Aniruddha Kembhavi, and Ranjay Krishna. Sugarcane: Fixing hackable benchmarks for vision-language compositionality. *Advances in neural information processing systems*, 36, 2024. [2, 3, 7](#)
- [11] Dieuwke Hupkes, Verna Dankers, Mathijs Mul, and Elia Bruni. Compositionality decomposed: How do neural networks generalise? *Journal of Artificial Intelligence Research*, 67:757–795, 2020. [2](#)
- [12] Justin Johnson, Bharath Hariharan, Laurens Van Der Maaten, Li Fei-Fei, C Lawrence Zitnick, and Ross Girshick. Clevr: A diagnostic dataset for compositional language and elementary visual reasoning. In *CVPR*, pages 2901–2910, 2017. [2, 3, 1](#)
- [13] Amita Kamath, Jack Hessel, and Kai-Wei Chang. Text encoders bottleneck compositionality in contrastive vision-language models. In *Proceedings of the 2023 Conference on Empirical Methods in Natural Language Processing*, pages 4933–4944, 2023. [2](#)
- [14] Amita Kamath, Jack Hessel, and Kai-Wei Chang. What’s “up” with vision-language models? investigating their struggle with spatial reasoning. In *Proceedings of the 2023 Conference on Empirical Methods in Natural Language Processing*, pages 9161–9175, 2023. [2](#)
- [15] Amita Kamath, Cheng-Yu Hsieh, Kai-Wei Chang, and Ranjay Krishna. The hard positive truth about vision-language compositionality. In *ECCV*, 2024. [2](#)
- [16] Martha Lewis, Nihal Nayak, Peilin Yu, Jack Merullo, Qinan Yu, Stephen Bach, and Ellie Pavlick. Does clip bind concepts? probing compositionality in large image models. In *Findings of the Association for Computational Linguistics: EACL 2024*, pages 1487–1500, 2024. [1, 2, 5](#)
- [17] Victor Weixin Liang, Yuhui Zhang, Yongchan Kwon, Serena Yeung, and James Y Zou. Mind the gap: Understanding the modality gap in multi-modal contrastive representation learning. *Advances in Neural Information Processing Systems*, 35:17612–17625, 2022. [8](#)
- [18] Tsung-Yi Lin, Michael Maire, Serge Belongie, James Hays, Pietro Perona, Deva Ramanan, Piotr Dollár, and C Lawrence Zitnick. Microsoft coco: Common objects in context. In *ECCV*, 2014. [3, 7, 2](#)

[19] Zixian Ma, Jerry Hong, Mustafa Omer Gul, Mona Gandhi, Irena Gao, and Ranjay Krishna. Crepe: Can vision-language foundation models reason compositionally? In *CVPR*, pages 10910–10921, 2023. [2](#)

[20] Leland McInnes, John Healy, and James Melville. Umap: Uniform manifold approximation and projection for dimension reduction. *arXiv preprint arXiv:1802.03426*, 2018. [8](#)

[21] Roni Paiss, Ariel Ephrat, Omer Tov, Shiran Zada, Inbar Mosseri, Michal Irani, and Tali Dekel. Teaching clip to count to ten. In *Proceedings of the IEEE/CVF International Conference on Computer Vision*, pages 3170–3180, 2023. [2](#)

[22] Shubham Parashar, Zhiqiu Lin, Tian Liu, Xiangjue Dong, Yanan Li, Deva Ramanan, James Caverlee, and Shu Kong. The neglected tails in vision-language models. In *CVPR*, pages 12988–12997, 2024. [2](#)

[23] Maitreya Patel, Abhiram Kusumba, Sheng Cheng, Changhoon Kim, Tejas Gokhale, Chitta Baral, and Yezhou Yang. Tripletcip: Improving compositional reasoning of clip via synthetic vision-language negatives. *arXiv preprint arXiv:2411.02545*, 2024. [3](#)

[24] Alec Radford, Jong Wook Kim, Chris Hallacy, Aditya Ramesh, Gabriel Goh, Sandhini Agarwal, Girish Sastry, Amanda Askell, Pamela Mishkin, Jack Clark, et al. Learning transferable visual models from natural language supervision. In *International conference on machine learning*, pages 8748–8763. PMLR, 2021. [1, 2](#)

[25] Arijit Ray, Filip Radenovic, Abhimanyu Dubey, Bryan Plummer, Ranjay Krishna, and Kate Saenko. Cola: A benchmark for compositional text-to-image retrieval. *NIPS*, 36, 2024. [2](#)

[26] Simon Schrödi, David T Hoffmann, Max Argus, Volker Fischer, and Thomas Brox. Two effects, one trigger: On the modality gap, object bias, and information imbalance in contrastive vision-language representation learning. *arXiv preprint arXiv:2404.07983*, 2024. [8](#)

[27] Yingtian Tang, Yutaro Yamada, Yoyo Zhang, and Ilker Yıldırım. When are lemons purple? the concept association bias of vision-language models. In *Proceedings of the 2023 Conference on Empirical Methods in Natural Language Processing*, pages 14333–14348, 2023. [1, 2, 5](#)

[28] Tristan Thrush, Ryan Jiang, Max Bartolo, Amanpreet Singh, Adina Williams, Douwe Kiela, and Candace Ross. Winoground: Probing vision and language models for visio-linguistic compositionality. In *Proceedings of the IEEE/CVF Conference on Computer Vision and Pattern Recognition*, pages 5238–5248, 2022. [1, 2, 3](#)

[29] Shengbang Tong, Erik Jones, and Jacob Steinhardt. Mass-producing failures of multimodal systems with language models. *NIPS*, 36, 2024. [2](#)

[30] Shengbang Tong, Zhuang Liu, Yuexiang Zhai, Yi Ma, Yann LeCun, and Saining Xie. Eyes wide shut? exploring the visual shortcomings of multimodal llms. In *CVPR*, pages 9568–9578, 2024. [2](#)

[31] Mert Yuksekgonul, Federico Bianchi, Pratyusha Kalluri, Dan Jurafsky, and James Zou. When and why vision-language models behave like bags-of-words, and what to do about it? In *ICLR*, 2023. [1, 2, 3, 6, 7, 5](#)

[32] Tian Yun, Usha Bhalla, Ellie Pavlick, and Chen Sun. Do vision-language pretrained models learn composable primitive concepts? *Transactions on Machine Learning Research*, 2023. [2](#)

[33] Tiancheng Zhao, Tianqi Zhang, Mingwei Zhu, Haozhan Shen, Kyusong Lee, Xiaopeng Lu, and Jianwei Yin. Vl-checklist: Evaluating pre-trained vision-language models with objects, attributes and relations. *arXiv preprint arXiv:2207.00221*, 2022. [2](#)

CLIP Behaves like a Bag-of-Words Model Cross-modally but not Uni-modally

Supplementary Material

8. Datasets

In this section, we provide details for the datasets introduced in Section 3.2. A summary of the key dataset characteristics for the CLEVR, PUG:SPAR, and PUG:SPARE is presented in Table 4.

8.1. CLEVR

Generation. Following the CLEVR dataset introduced in [12], we generate new images using the 3D modeling software Blender [7]. The dataset contains images with M colored objects and corresponding captions. The set of objects is $\mathcal{O} = \{\text{cube, sphere, cylinder}\}$, and the attributes are selected from the set of eight colors: $\mathcal{A} = \{\text{blue, red, purple, cyan, gray, brown, green, yellow}\}$.

The data generation process is shown in Fig. 8. We randomly sample objects and attributes to create combinations of M objects of various attributes. For example, an attribute-object combination of 5 objects is 2 blue cubes, 1 green sphere, 1 purple sphere, and 1 blue cylinder. For scenes with two objects, we enforce that the objects are distinct. This results in 192 unique combinations of two objects: 3 choices for the first object, 2 for the second, 8 color options per object (colors can repeat), divided by 2 to ignore object order: $3 \times 2 \times 8 \times 8 \times 0.5 = 192$

Using the original CLEVR image generation pipeline, we construct a scene in Blender based on the sampled combinations. Objects are placed randomly on a neutral background with variations in material and size. The rendered images have dimensions of 320×240 . For captions, we concatenate the attributes and objects in the format: “ $a_1 o_1$ and $a_2 o_2$ and ... and $a_M o_M$ ” where $a_j \in \mathcal{A}$ and $o_j \in \mathcal{O}$ for $j \in 1, \dots, M$.

We generate $N = 5000$ samples for each M -object configuration. For the experiments in Sections 3.4 and 4, we use $M = 2$. For testing uni-modal binding with an increasing number of objects in Section 5.1, we consider M ranging from 2 to 10. Sample images and captions are shown in Fig. 9.

Train/test split. For each M -object setting, we divide the dataset into training, validation, and test sets in a 90/10/10 ratio based on attribute-object combinations. For instance, if there are 192 attribute-object combinations for the two-object setting, 19 combinations are assigned to the validation set, 19 to the test set, and the remaining combinations to the training set. This ensures that the same combination does not appear in both the training and test sets.

8.2. PUG:SPAR

Description. PUG:SPAR is a synthetically generated dataset in Unreal Engine [6], featuring animal figures on various backgrounds. The animals can have their natural colors or attributes such as red, blue, grass, and stone. For our project, which tests attribute-object relationships in a controlled environment, we filter the dataset to include scenes with two animals and annotated attributes. This leaves us with images of two objects either in a blue/red or grass/stone attribute setting, with one animal on the left and the other on the right. However, the attributes are fixed to positions: the left objects are always blue or grass, and the right objects are always red or stone. This results in $32 \times 31 \times 2 = 1984$ attribute-object combinations and a total of 19840 images.

As discussed in Section 3.2, the fixed relationship between attributes and positions could lead to a shortcut strategy for the linear classifier: first identifying the blue/red or grass/stone setting, and then determining if the target object is on the left or right. To address this, we create PUG:SPARE, a dataset with an extended set of attributes that are independent of object positions.

Train/test split. Similar to the CLEVR dataset, we split the dataset into training, validations, and test sets based on attribute-object combinations in a 90/10/10 ratio.

8.3. PUG:SPARE

Generation. Similar to PUG:SPAR, we generate photorealistic images of two animals on different backgrounds. Our dataset includes 12 possible animal objects and 8 possible colors for these animals. The objects appear in 4 different environments, creating varied backgrounds and lighting conditions. The relative positions between the two objects also change: the left object in front and the right object in the back, the left object in the back and the right object in front, and both objects at the same distance. Animals and attributes do not repeat. For example, “red zebra and blue lion” is valid. However, “red zebra and red lion” or “red zebra and blue zebra” are not. We generate all possible two-object combinations with these conditions. This results in 12 choices for the first object, 11 choices for the second object, 8 colors for the first object, 7 colors for the second object, divided by 2 to ignore the order: $12 \times 11 \times 8 \times 7 \times 0.5 = 3696$ combinations.

The images for these combinations are rendered in Unreal Engine. The image dimensions are 512×512 . Captions follow the form “ $a_1 o_1$ and $a_2 o_2$ ”, where $a_j \in \mathcal{A}$ and $o_j \in \mathcal{O}$. The examples are shown in Fig. 10.

	CLEVR	PUG:SPAR	PUG:SPARE
#images	5000	19840	88704
#attribute-objects combinations	192	1984	3696
#objects	3	32	12
#attributes	8	4	8
#backgrounds	1	10	4
positions	random	{left, right}	{left, right} \times {front, back, equal}

Table 4. **Specifications for the datasets used to test attribute-object binding in a controlled setting.** For CLEVR, the number of attribute-object combinations only reflects the two-object case. For PUG:SPAR, the numbers represent the filtered dataset used in our experiments.

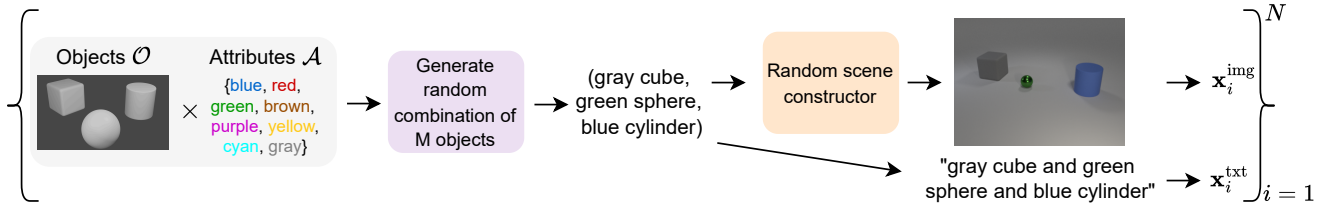


Figure 8. **CLEVR dataset generation process.** From a set of objects and attributes, we randomly generated combinations of M objects per scene. Each combination was rendered with Blender, and a caption was generated by concatenating attributes and objects to match the image.

Train/test split. Similar to the CLEVR dataset, we divide the dataset into train, validation, and test splits based on the attribute-object combinations.

8.4. COCO, ARO, SugarCrepe

We evaluate the cross-modal binding performance of our method on real-world datasets by training on COCO [18]. Following the protocol in [31], we apply the Karpathy splits to divide the dataset into train, validation, and test sets.

The trained models are then assessed on compositional benchmarks, ARO [31] and SugarCrepe [10]. Examples from these benchmarks are shown in Fig. 11.

9. Discussion on establishing BoWness

Previous studies evaluating CLIP’s Bag-of-Words (BoW) behavior have typically combined both text and image modalities, following the standard zero-shot learning approach. These assessments generally fall into two categories. The first approach, as demonstrated in [16, 27], involves comparing images to captions that describe only a single object in the scene. For example, given an image with a yellow sphere and a red cube, the text prompts might be: ‘a photo of {yellow sphere, yellow cube, red sphere, blue cube, purple cylinder}’ (Fig. 12(a)). We argue that focusing on single-object descriptions does not fully capture CLIP’s capability for compositional reasoning in multi-object contexts. Since CLIP is trained to match an image to the caption that best aligns with its content, ‘yellow cube’ would be a better match than ‘yellow sphere’ in this example, as it

provides a more accurate representation of the concepts in the scene. Limiting the evaluation to single-object descriptions, therefore, does not fairly test its ability to understand attribute-object associations.

The second approach, seen in studies like [31], provides a more robust evaluation by comparing a query image to permutations of a more complete description, effectively testing BoWness. We adopt this methodology for our experiments in Section 3.3. Specifically, we measure CLIP’s accuracy in choosing between correct and permuted captions. For CLEVR, if the correct caption is ‘yellow sphere and red cube’, we compare it to its permutation, ‘red sphere and yellow cube’ (Fig. 12(b)). Similarly, for the PUG:SPAR and PUG:SPARE datasets, we test the model’s ability to distinguish between captions like ‘blue elephant and red lion’ versus ‘red elephant and blue lion’ (Fig. 12(c),(d)).

10. Details for uni-modal binding

In this section, we provide details about the experiments conducted in Section 3.4.

Since each linear probe is object-specific, we filter the dataset to include only examples containing the target object. These examples are split into training, validation, and test sets with a 90/10/10 ratio based on the attribute-object combinations that include the target object.

We use OpenAI’s CLIP model for all experiments [24]. The main results presented in Table 1 are based on the ViT-L/14 model, while additional results with the ViT-B/32 and ViT-B/16 models are shown in Table 5. During linear prob-

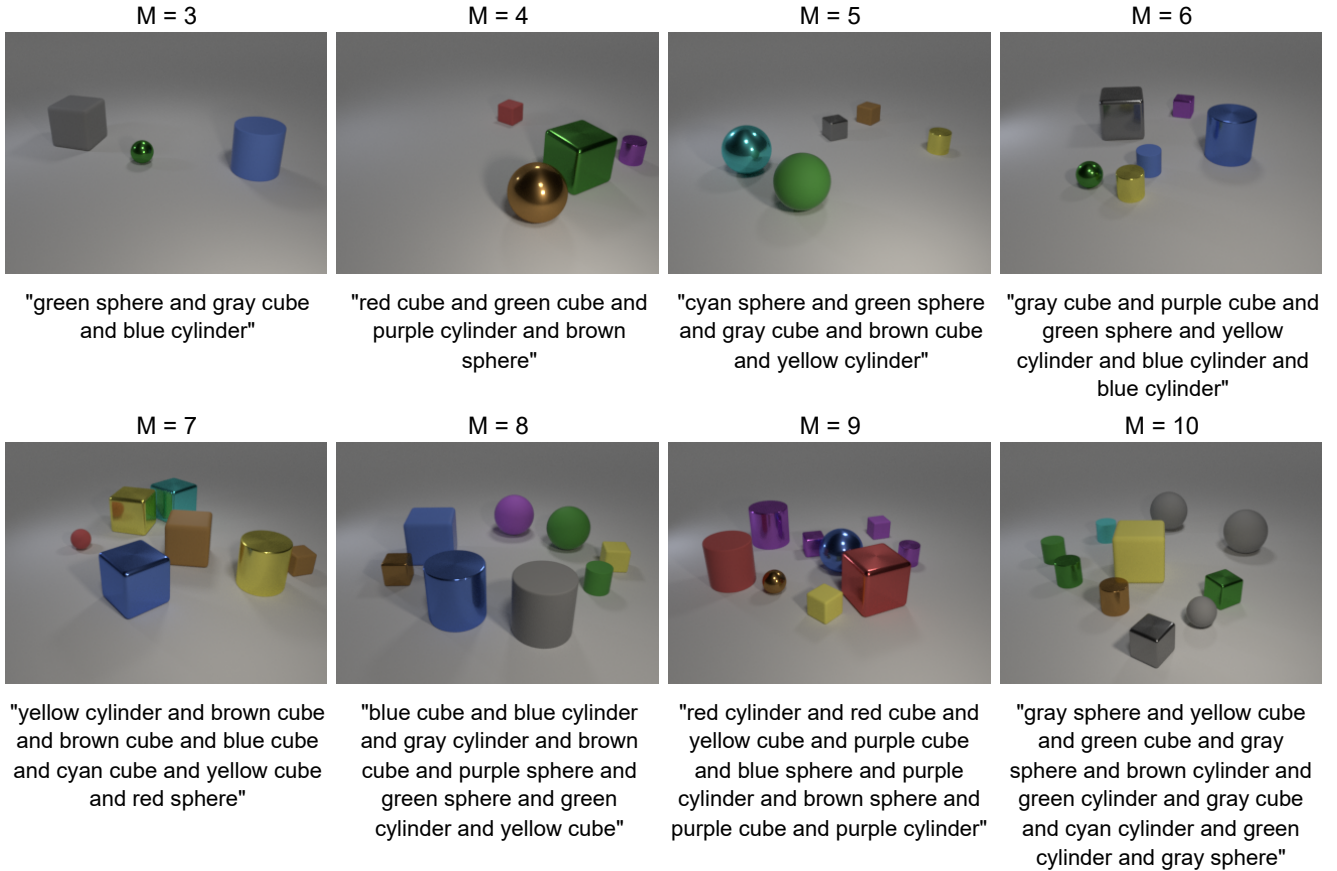


Figure 9. **Scene complexity increases with more objects.** We show examples from the CLEVR dataset with scenes containing different numbers of objects to highlight how image and text complexity changes with object count.



Figure 10. **PUG:SPARE dataset examples.** PUG:SPARE offers all possible configurations of two objects from the set of 12 objects, 8 attributes, 4 backgrounds, and 3 position configurations (front/back, back/front, at the same distance). This allows comprehensive testing of attribute-object binding.

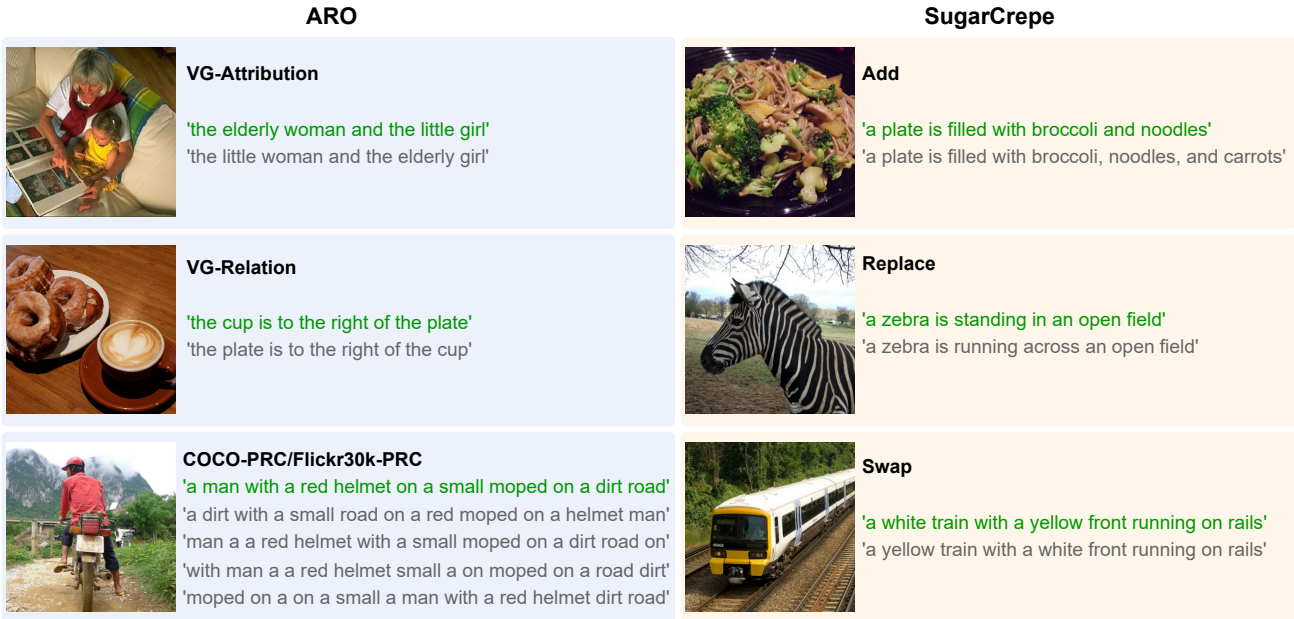


Figure 11. **Examples from the compositional benchmarks ARO and SugarCrepe.** These datasets are designed to test VLMs’ ability to accurately bind attributes and objects in complex, real-world scenarios. The images illustrate varied compositions of objects, attributes, and their relationships, challenging a model’s compositional understanding.

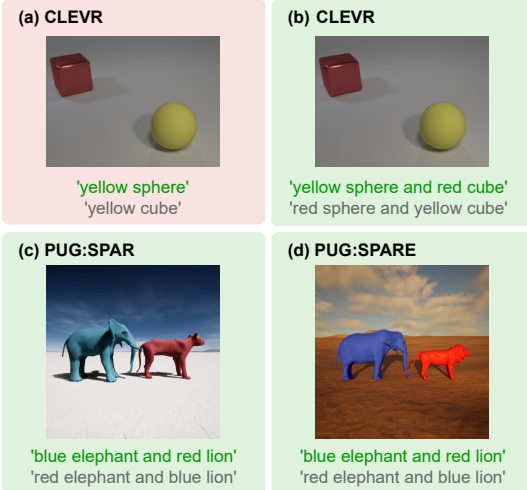


Figure 12. **Illustrating BoWness.** The figure presents examples from CLEVR, PUG:SPAR, and PUG:SPARE datasets, used to demonstrate BoWness. The highlighted example in red shows a case where an image is compared to captions describing only a single object, which can lead to inaccurate assessments due to incomplete scene information.

ing, the model weights are frozen. For upper-bound results derived with fine-tuning, we unfreeze the relevant image or text encoder weights and allow them to update during training. All models are trained on a single Nvidia A100 GPU.

We do not normalize the image or text embeddings before passing them to the linear classifiers. The linear classifiers are implemented in PyTorch using cross-entropy loss. Accuracy is measured by predicting attributes and averaging the results across all object-specific classifiers. In the two-object case, each object has only one possible color, and the task is to predict a single color per object. In the multi-object case, where multiple instances of the target object may appear, a prediction is considered correct only if all colors for the given target object are accurate.

We use both manual and random searches for hyperparameter tuning. A batch size of 32 consistently performs well across all datasets. For CLEVR, linear probing without fine-tuning requires learning rates of $\{0.1, 0.01, 0.001\}$ and training for 1000 to 5000 epochs for images or 200 to 1000 epochs for text. For fine-tuning, we reduce the number of epochs to a range of 5 to 20. For the PUG datasets, we maintain a batch size of 32, with a learning rate of 0.1, and train for 50 to 200 epochs when not fine-tuning. For fine-tuning, the learning rates range between 0.001 and 0.01, with 5 to 50 epochs. Both training regimes utilize the SGD optimizer. The optimal configurations are selected based on validation set accuracy.

Details on training a BoW model. We simulate a BoW model by training CLIP encoders to recognize all attributes in the input while ignoring binding to objects.

We attach a linear layer to CLIP’s image or text encoder that maps to attribute classes, similar to linear probes. We

Dataset	Encoder	Image		Text	
		Train	Test	Train	Test
CLEVR	ViT-B/32	1.0	0.91	1.0	0.99
	ViT-B/16	1.0	0.90	1.0	0.99
PUG:SPAR	ViT-B/32	1.0	0.97	1.0	0.98
	ViT-B/16	1.0	0.98	1.0	0.99
PUG:SPARE	ViT-B/32	0.96	0.90	1.0	0.99
	ViT-B/16	0.96	0.92	1.0	0.99

Table 5. **CLIP is not BoW uni-modally.** We evaluate the attribute-object binding information in CLIP’s image and text embeddings. The table shows the accuracies of linear probes classifying attributes for each target object, averaged across all objects. The table extends Table 1 with results for ViT-B/32 and ViT-B/16 backbones. Pre-trained CLIP encoders contain sufficient binding information within each modality.

then reinitialize the CLIP encoders randomly and train the model to predict all attributes in the input with soft label cross-entropy loss. The soft labels correspond to the normalized count of attributes in the input. This ensures that the model behaves as a BoW because it is tasked to predict attributes without having to link them to specific objects. We use these newly trained CLIP embeddings and apply linear probing to evaluate the presence of attribute-object binding information.

As explained in the main text, such a BoW model does not achieve high linear probing accuracy. On CLEVR, the average test accuracies of the linear probes are 0.66 for images and 0.85 for text, significantly worse than the probing performance on the actual CLIP embeddings (0.96). This reinforces the idea that BoW models do not contain features that are useful for binding.

11. Cross-modal binding details

In this section, we provide additional details about LABCLIP, discussed in Section 4.

We use OpenAI’s CLIP for all experiments, specifically the L/14 model for CLEVR, PUG:SPAR, and PUG:SPARE, as shown in Table 2. Additional results for the B/32 and B/16 models are provided in Table 6. All models were trained using a single Nvidia A100 GPU.

The LABCLIP method involves adding an additional linear layer to the text encoder while keeping the CLIP weights frozen. For the upper bound results with fine-tuned CLIP, we unfreeze both encoder weights. The additional linear layer has the same dimension as the network output, equivalent to multiplying by a $D \times D$ matrix. We initialize this matrix as an identity matrix, which corresponds to the case when no transformation is applied.

We use the same contrastive loss as in the original CLIP. The temperature parameter in the contrastive loss is a learn-

Model	Backbone	Accuracy		Recall@1	
		Train	Test	Train	Test
CLEVR					
CLIP	ViT-B/32	0.52	0.49	0.33	0.34
LABCLIP-SB	ViT-B/32	0.99	0.85	0.99	0.83
LABCLIP-HNB	ViT-B/32	0.99	0.83	0.99	0.81
CLIP	ViT-B/16	0.50	0.54	0.31	0.38
LABCLIP-SB	ViT-B/16	1.00	0.93	1.00	0.92
LABCLIP-HNB	ViT-B/16	1.00	0.93	1.00	0.92
PUG:SPAR					
CLIP	ViT-B/32	0.51	0.51	0.02	0.02
LABCLIP-SB	ViT-B/32	0.99	0.97	0.93	0.83
LABCLIP-HNB	ViT-B/32	0.99	0.98	0.93	0.84
CLIP	ViT-B/16	0.52	0.53	0.04	0.04
LABCLIP-SB	ViT-B/16	0.99	0.97	0.94	0.88
LABCLIP-HNB	ViT-B/16	1.00	0.98	0.95	0.89
PUG:SPARE					
CLIP	ViT-B/32	0.51	0.51	0.01	0.01
LABCLIP-SB	ViT-B/32	0.91	0.89	0.73	0.69
LABCLIP-HNB	ViT-B/32	0.95	0.93	0.77	0.73
CLIP	ViT-B/16	0.51	0.50	0.03	0.03
LABCLIP-SB	ViT-B/16	0.91	0.87	0.84	0.80
LABCLIP-HNB	ViT-B/16	0.96	0.92	0.88	0.84

Table 6. **LABCLIP enhances cross-modal binding.** These results extend the findings shown in Table 2 for ViT-B/32 and ViT-B/16 backbones.

able parameter, initialized to 0. The **Standard Batch** contains only the corresponding images and text in each batch, while the **Hard Negative Batch** also includes hard negative captions. For synthetic datasets, we obtain hard negatives by swapping attributes. For COCO, we utilize the attribute and noun shuffling method introduced in NegCLIP to create negative captions [31]. For example, in COCO-PRC example shown in Fig. 11, when the correct caption is ‘a man with a red helmet on a small moped on a dirt road’, a possible negative caption is ‘a dirt with a small road on a red moped on a helmet man’. There are no negative images in our approach.

We employ a combination of manual and random searches for hyperparameter tuning, with the batch size ranging from 32 to 2048, epochs from 5 to 50, and learning rates between 0.0001 and 0.01. We use the Adam optimizer for LABCLIP but SGD when fine-tuning on the CLEVR and PUG datasets. The optimal hyperparameters are selected based on the final epoch performance on the validation set.